

Green Synthesis of Silver Nanoparticles: Synthesis, Characterization and Antibacterial Activity

Thanaa I. Shalaby¹, Ola A. Mahmoud², Gihaan A. El Batouti^{3,*}, Ebtihag E. Ibrahim¹

¹Department of Medical Biophysics, Medical Research Institute, Alexandria University, Alexandria, Egypt

²Department of Microbiology, Medical Research Institute, Alexandria University, Alexandria, Egypt

³Department of Microbiology and Immunology, Faculty of Pharmacy, Pharos University, Alexandria, Egypt

Abstract The synthesis of metal and semiconductor nanoparticles is an expanding research area due to the potential applications for the development of novel technologies. In this work, we describe a cost effective and environment friendly technique for green synthesis of silver nanoparticles and evaluate their antibacterial activity from silver nitrate solution through the extract of *Zingiber officinale* rhizome as a reducing as well as a capping agent. The growth of nanoparticles was monitored by UV-vis spectrophotometer and complemented with characterization using Transmission Electron Microscopy, X-ray Diffraction and Fourier Transform Infrared Spectroscopy. Transmission Electron Microscopy revealed the presence of mono-dispersed silver nanoparticles with an average size of 3.1 nm. X-ray diffraction studies corroborated that the biosynthesized nanoparticles were crystalline silver. Fourier Transform Infra-Red spectroscopy analysis showed that the synthesized nano- silver were capped with bimolecular compounds which were responsible for the reduction of silver ions. The antibacterial effect of these nanoparticles were studied against *Staphylococcus aureus* and *Escherichia coli*. This study indicated that silver nanoparticles posses considerable antibacterial activity in comparison with standard antibacterial agents, and hence further investigation or clinical applications is necessary.

Keywords Antibacterial activity, Fourier Transform Infra-Red Spectroscopy, Green synthesis, Silver nanoparticles, X-Ray Diffraction, *Zingiber officinale*

1. Introduction

Nanotechnology can be termed as the synthesis, characterization, exploration and application of nano-sized (1-100nm) materials for the development of science. It deals with the materials whose structures exhibit significantly novel and improved physical, chemical, and biological properties. Nanotechnology holds a promising future for the design and development of many types of novel products that are used in early detection, treatment, and prevention of various diseases. [1]

Synthesis and characterization of nanoparticles is an emerging field for research. Preparation of nanoparticles requires processes that include chemical and physical techniques. With the development of several chemical-synthetic techniques, the concern for environmental contamination is also heightened as the protocols used for chemical synthesis require some toxic chemicals for their synthesis. Most physical methods deal with enormous consumption of energy to maintain the high

pressure and temperature employed in the synthesis procedures. To overcome these chemical and physical hazards, the adoption of green chemistry has been pursued to minimize bio-hazardous waste. [2] The use of environmentally friendly material as plant extracts, bacteria and fungi offers numerous benefits of eco-friendliness and compatibility for pharmaceutical and biomedical applications. [3, 4]

Due to their exclusive properties, silver nanoparticles (Ag-NPs) may have several applications, including their use as catalysts, [5] as optical sensors, in spectrally selective coatings for absorption of solar energy, [6] in textile engineering, in electronics, [7] and most importantly in the medical field as a bactericidal and as a therapeutic agent. [8, 9] Ag-NPs have high reactivity due to the large surface to volume ratio and play a crucial role in inhibiting bacterial growth in aqueous and solid media. [10] The investigation of this phenomenon has regained importance due to the increase of bacterial resistance to antibiotics. Ag-NPs obtained by methods conveying green synthesis are candidates to be used in biological systems. [11].

The aim of this work was to study the synthesis and characterization of Ag-NPs using *Zingiber officinale* rhizome extracts as a reducing and capping agent (green pathways). Their antibacterial activity was also evaluated.

* Corresponding author:

g_infcont@hotmail.com (Gihaan A. El Batouti)

Published online at <http://journal.sapub.org/nn>

Copyright © 2015 Scientific & Academic Publishing. All Rights Reserved

2. Material and Methods

2.1. Preparation of the Reagent

Silver nitrate (AgNO_3) was purchased from Sigma Aldrich and fresh ginger rhizome (*Zingiber officinale*) was purchased from a local market. A 10 gm of thoroughly washed ginger rhizome was used to prepare the extract. The upper part was removed by a knife, chopped into the fine pieces and converted into a paste using mortar-pestle. This was followed by the addition of 40 ml deionized water, that was boiled for 2 minutes and filtered, then centrifuged at 5000 rpm for 15 minutes. The supernatant was collected to be further used as ginger rhizome broth for the experiment.

2.2. Synthesis of Ag-NPs

A 50 ml of 1mM silver nitrate (AgNO_3) was heated to boiling. To this solution, 10 ml of ginger rhizome broth was added for reduction of silver ions (Ag^+), then kept at room temperature for one hour. The color transformation from yellow to yellowish brown indicated the formation of Ag-NPs. [12]

2.3. Characterization of Ag-NPs: [13, 14, 15]

The color change in reaction mixture (metal ion solution and ginger extract) was recorded through visual observation. The bio-reduction of Ag^+ in aqueous solution was monitored by measuring the spectrum of the solution within the range of 350–600 nm using UV-Vis-spectrophotometer (Unicam UV5-220), and a quartz cuvette with water as the reference. To study the stability of nanoparticles colloidal solution, the solution was kept at room temperature for one week. During this period UV-Vis spectrum of the solution was measured at different time intervals; after half hour, 24hrs and one week. The color and pH of the solution were also checked at regular intervals, which hardly showed any change. The size and morphology of the nanoparticles were examined using a transmission electron microscope (TEM, JEOL 100 CX). The sample was prepared by placing a drop of Ag-NPs on a carbon-coated copper grid and was then left to dry in air, before transferring it to the microscope. The crystalline nature of Ag-NPs was analyzed by X-ray diffractometer (Shimaduz, XRD- 7000, Maxima, Japan), operated at a voltage of 30 KV, a current of 30 mA, with $\text{CuK}\alpha$ radiation and analyzed between 5 and 100° (2θ). The crystallite domain size was calculated from the width of the XRD peaks, assuming that they were free from non-uniform strains, using the Scherrer's equation as follows:

$$D = 0.94 \lambda / \beta \cos \theta \quad (1)$$

where D is the average crystallite domain size perpendicular to the reflecting planes, λ is the X-ray wavelength, β is the full width at half maximum (FWHM), and θ is the diffraction angle. After the complete reduction of Ag^+ ions by the ginger rhizome extract, 10 ml solution of Ag-NPs was centrifuged at 4000 rpm for 10 min and the resulting suspension was re-dispersed into 20 ml of deionized water. The process of centrifuging and re-dispersing was repeated three times to

render nanoparticles free from proteins or other bioorganic compounds that may be present in the solution. Then, the purified suspension was completely dried in a lyophilizer, diluted with potassium bromide in the ratio of 1:100, and analyzed by Fourier Transform Infrared (FTIR) spectroscopy (Shimadzu IR Prestige-21) with a diffuse reflectance mode (DRS-8000) attachment. All measurements were carried out in the range of 400–4000 cm^{-1} at a resolution of 4 cm^{-1} .

2.4. Antibacterial Assay

The antimicrobial susceptibility of green synthesized Ag-NPs was evaluated using the disc diffusion method and growth inhibition test. Pure slant cultures of *Staphylococcus aureus* (*S.aureus*) and *Escherichia coli* (*E.coli*) were obtained from the Microbiology Department of the Medical Research Institute (MRI) Alexandria, Egypt. [16]

2.4.1. Disc Diffusion Method

Bauer-Kirby's disc diffusion method was used. Müller-Hinton Agar was prepared from a commercially available dehydrated medium (Oxoid®) according to manufacturer's instructions. The dried surface of Mueller-Hinton agar plates were inoculated with two pathogenic bacterial strains; one with a Gram-positive bacteria, *S.aureus* and one with a Gram-negative bacteria, *E. coli* by swabbing over the entire sterile agar surface. Sterile paper discs made of Whatman filter paper (Np:1), 6 mm in diameter were loaded with Ag-NPs (50 μL , 3mM). Two standard antibiotic discs; *Gentamycin* and *Ciprofloxacin* (Oxoid®), were also placed in each plate to be used as control antibiotics. The cultured agar plates were incubated at 37°C for 24 hours, after which the zones of inhibition were observed.

2.5. Estimation of Colony Forming Units

E.coli was used for the estimation of colony forming units (CFU) on solid agar plates. Freshly grown bacterial inoculum of (10^5 cells/ml) of *E.coli* was inoculated into tubes containing 500 μL liquid Tryptone Soy Broth medium (T.S.B). They were left to grow in a shaking incubator at 37°C, with 200 rpm for 3 hours. The tubes were then treated with different concentrations of Ag-NPs (0, 20, 40, 60 $\mu\text{g/ml}$). These samples were diluted at 10^6 folds to obtain better discrete colonies, and were thereafter spread on nutrient agar plates. After incubation at 37°C for 24 hours, the numbers of CFU were observed.

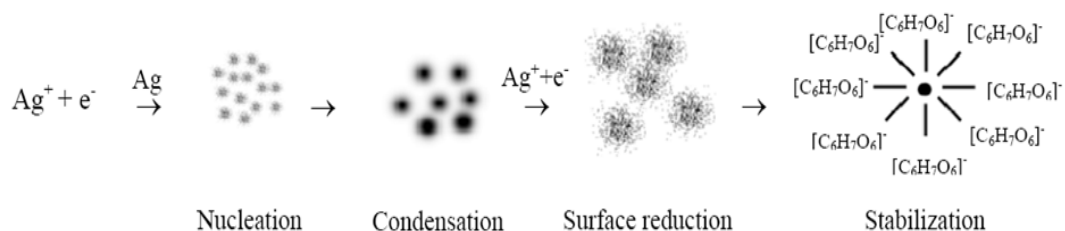
3. Results and Discussion

In this study, ginger was as biological system for the synthesis of Ag-NPs. Oxalic acid, ascorbic acid, phenyl-propanoids and zingerone are present in the chemical composition of ginger [17]. Ascorbic acid and/or oxalic acid are/is the main organic components in the extract which play(s) the role of reducing Ag^+ into Ag-NPs. The possible stages of the formation of Ag-NPs from ginger extract during

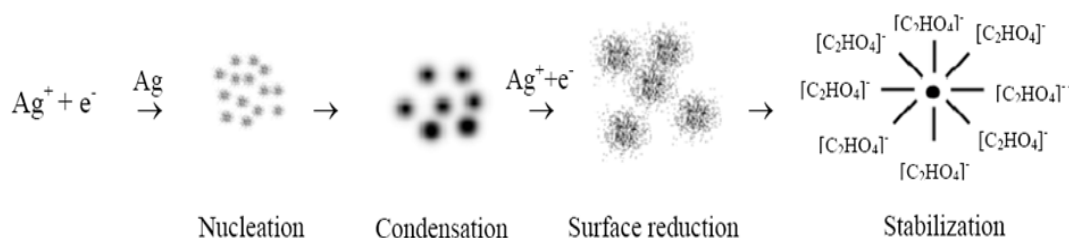
the chemical reaction included nucleation, condensation, surface reduction and stabilization as illustrated in Figure 1.

It appears that oxalic acid ($C_2H_2O_4$) and/or ascorbic acid ($C_6H_8O_6$) present in ginger are/is chemically reduced in the presence of the colloidal solution containing Ag^+ ions of $AgNO_3$. The chemical reduction causes electron transfer, which converts Ag^+ ions to Ag , and results in the nucleation of particles. The availability of more Ag-NPs during this process, renders them to condense into bigger particles. As soon as these particles are formed, they are bound by the

layer (s) of oxalic acid and/or ascorbic acid through electrostatic forces of the ginger extract. In addition to the above reducing acids there are other components like zingerone and phenyl- propanoids in the phytochemicals of the ginger extract. Zingerone ($C_6H_8O_6$) is a heterocyclic component which also aggregates along with other compounds, around the layers of reducing acids and consequently acts as a protective material for the stabilization of Ag-NPs.



Scheme (1)



Scheme 2

Figure 1. Two schemes represent the possible stages of the formation of Ag-NPs from ginger extract

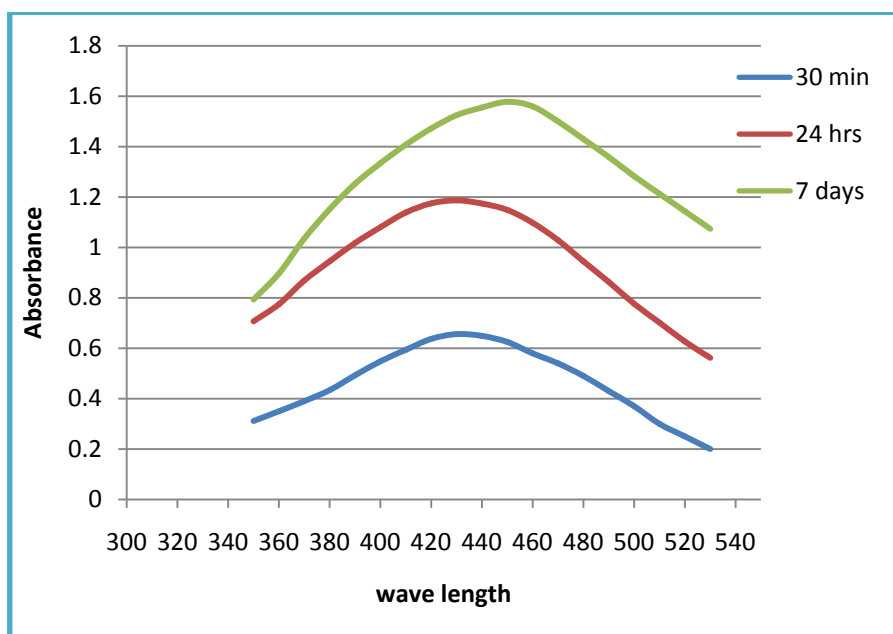


Figure 2. UV-vis absorption spectra recorded as function of time for silver nanoparticles using rhizome extract of *Zingiber officinale*

3.1.2. Confirmation of Ag-NPs by XRD

XRD is a very important technique that is commonly used to analyze the characteristics and structural details of nanomaterials. The XRD patterns are obtained by measuring the angles at which an X-ray beam is diffracted by the crystalline phases in the specimen. The XRD pattern of green synthesized Ag-NPs is shown in figure 4, where four prominent peaks at 38° (2θ); 44° (2θ); 64° (2θ) and 77° (2θ) indicated the presence of (111), (200), (220) and (311) sets of lattice planes, and accordingly could be indexed as

face-centered-cubic structures of Ag-NPs. Hence, from the XRD pattern it is clear that Ag-NPs formed using ginger rhizome broth were essentially crystalline in nature. The average crystalline particle size for green synthesized Ag-NPs determined by Scherrer's formula using the half width of the most intense XRD peaks was 4.17 ± 1.12 nm. It can be noted that the size of the Ag-NPs obtained from TEM is in agreement with the size obtained from the XRD measurements.

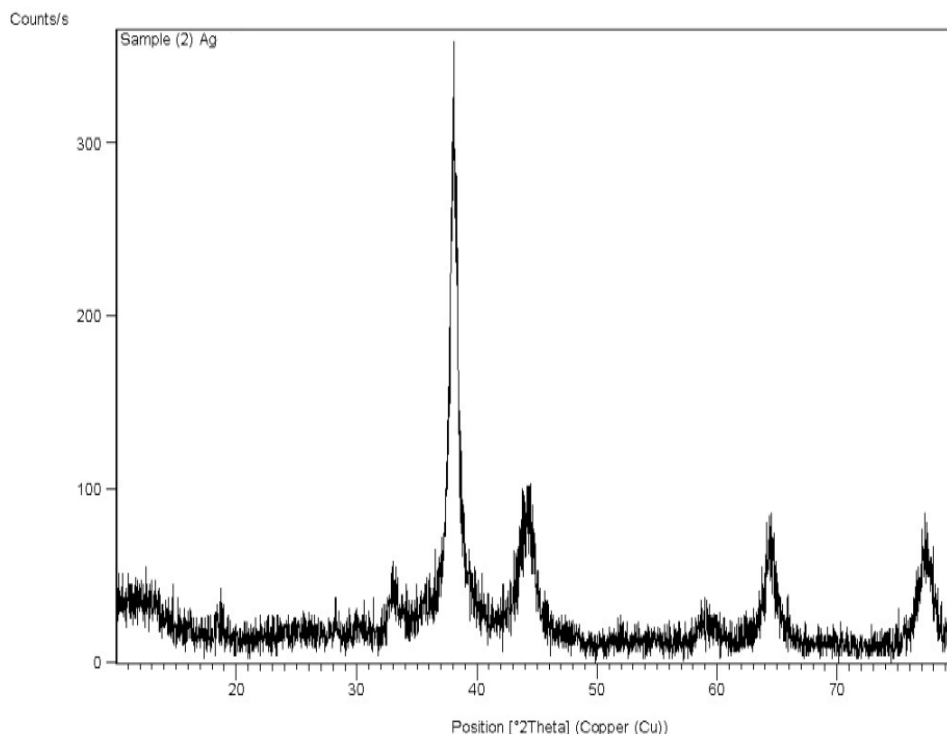


Figure 4. XRD spectrum of green synthesized of Ag-NPs using *Zingiber officinale* extract

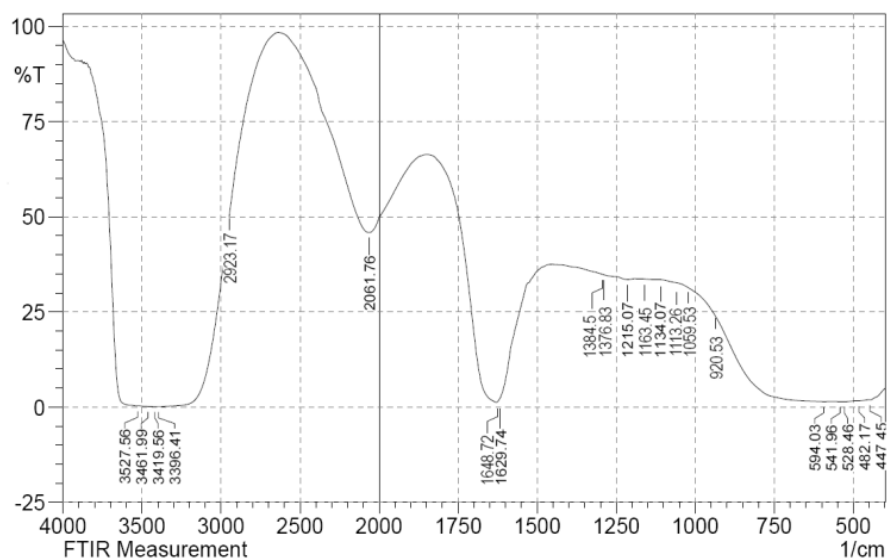


Figure 5. FTIR spectrum of the Ag-NPs synthesized by the reduction of AgNO_3 using *Zingiber officinale* extract

3.1.3. Mechanism of Formation of Ag-NPs by FTIR

FTIR measurements were performed to identify the potential biomolecules in the ginger rhizome responsible for the reduction and then provision of stability to the bio-reduced Ag-NPs. Figure 5 displays the FTIR spectra of Ag-NPs; where the peak was centered at 1384 cm^{-1} which indicated the presence of NO_3^- in the residual solution. The band at 3419 cm^{-1} corresponds to O-H stretching H-bonded alcohols and phenols. The peak at 2923 cm^{-1} corresponds to O-H stretch carboxylic acids. The assignment at 1648 cm^{-1} corresponds to N-H bend primary amines. The peak at 1376 cm^{-1} corresponds to C-N stretching of aromatic amine group and the bands observed at 1163 , 1113 , 1059 cm^{-1} corresponds to C-N stretching alcohols, carboxylic acids, ethers and esters. The various functional groups mentioned here are mainly derived from heterocyclic compounds that are the water soluble components of ginger rhizome. So it can be assumed that different water soluble heterocyclic compounds such as alkanoids and flavonoids functioned as the capping ligands for the synthesis of Ag-NPs [18].

3.2. Antibacterial Activity of Ag-NPs

Antibacterial effect of Ag-NPs was studied against two different pathogenic bacteria; *S.aureus* and *E.coli* strains.

3.2.1. Antibacterial Assay of Ag-NPs

The effect of Ag-NPs on bacteria was performed using disc diffusion method. As shown in figure 6; larger clear inhibition zones surrounded the discs impregnated with Ag-NPs ($50\mu\text{L}$, 3mM) as compared to the standard control antibiotics used.

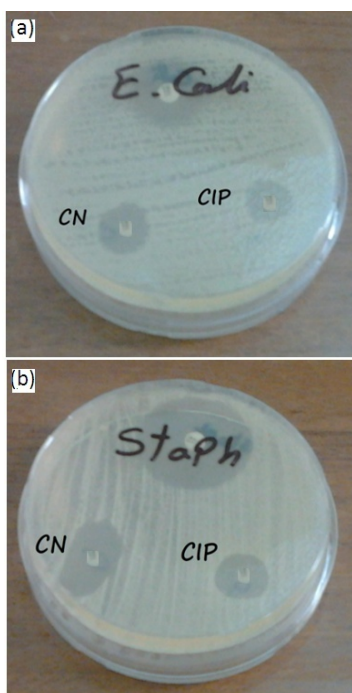


Figure 6. Antibacterial activity of 3mM Ag-NPs solution green synthesized by ginger extract (upper disc) and Gentamycin (CN), and Ciprofloxacin (CIP) used against, *E. coli* (a) and *S. aureus* (b)

3.2.2. Estimation of CFU

Figure 7 shows the plot of number of bacterial colonies grown on nutrient agar plates as a function of concentration of Ag-NPs. The colony count was significantly reduced with the increasing concentrations of Ag-NPs.

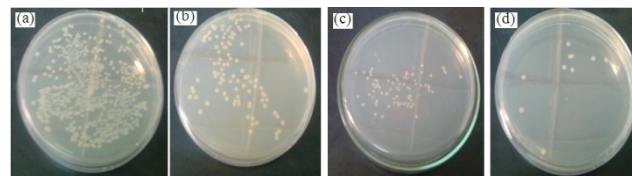


Figure 7. Digital photographs of *E. coli* colonies grown on nutrient agar plate as a function of silver nanoparticles concentration. a) Control, b) $20\text{ }\mu\text{g/ml}$, c) $40\text{ }\mu\text{g/ml}$ and d) $60\text{ }\mu\text{g/ml}$

Although the exact mechanism for inhibition of bacterial growth by Ag-NPs has not yet been elucidated, many possible mechanisms have been proposed. In general, positively charged silver ions from nanoparticles are believed to become attached to the negatively charged bacterial cell wall resulting in its rupture, leading to denaturation of proteins and finally cell death [19]. The attachment of either Ag ions or nanoparticles to the cell wall causes accumulation of envelope protein precursors, which results in dissipation of the proton motive force. Ag -NPs also exhibit destabilization of the outer membrane and rupture of the plasma membrane, thereby causing depletion of intracellular ATP. Ag- NPs are known to have an antimicrobial activity against Gram-negative bacteria, creating “pits” in the cell wall. Metal depletion may cause the formation of irregularly shaped pits in the outer membrane and alter the membrane’s permeability, which is due to the progressive release of lipopolysaccharide molecules and membrane proteins [20]. Another proposed mechanism involves the association of silver with oxygen and its reaction with sulfhydryl ($-\text{S}-\text{H}$) groups on the cell wall to form $\text{R}-\text{S}-\text{S}-\text{R}$ bonds, thereby blocking respiration and causing cell death [21]. Smaller Ag - NPs possess a larger surface area rendering it available for interaction thus producing a greater bactericidal effect than the larger Ag-NPs [22]. It is also possible that Ag-NPs not only interact with the surface of the membrane, but can also penetrate inside the bacteria. Silver ions can also interact with the DNA of bacteria, preventing cell reproduction [19].

4. Conclusions

Plants or their extracts can be efficiently used in the synthesis of Ag-NPs as a greener route. Control over the shape and size of nanoparticles seems to be very easy with the use of plants. In the present study we found that ginger rhizome may be a good source for the synthesis of Ag-NPs. This green approach for synthesis of Ag-NPs has many advantages such including the ease with which the process can be scaled up and its economic viability.

The use of such eco-friendly nanoparticles as a

bactericidal agent in medical and electronic applications, renders this method potentially exciting for a large-scale synthesis of other inorganic materials (nanomaterials).

REFERENCES

- [1] El-Nour K.M, Eftaiha A, Al-Warthan A, and Ammar R.A. 2010. Synthesis and applications of silver nanoparticles. *Arab J Chem*; 3, pp.135–140.
- [2] Shamim N and Sharma V.K Green Nanotechnology: Development of Nanomaterial for Environmental and Energy Applications. Chap 12 in *Sustainable Nanotechnology and the Environment: Advances and Achievements*, 2013.Vol. 1124. pp 201–229. American Chemical Society .ISBN13: 9780841227842.
- [3] Savithramma N, Rao M.. L, Rukmini K and Devi P.S. 2011, Antimicrobial activity of silver nanoparticles synthesized by using medicinal plants. *Int J Chem Tech Res*, 3 (3) 1394–1402.
- [4] Banerjee P, Satapathy M, Mukhopahayay A and Das P. 2014. Leaf extract mediated green synthesis of silver nanoparticles from widely available Indian plants: synthesis, characterization, antimicrobial property and toxicity analysis. *Bioresources and Bioprocessing*. 1:3 <http://www.bioresourcsbioprocessing.com/content/1/1/3>.
- [5] Santos K.O, Elias W.C, Signori A.M, Fernando C, Giacomelli F.C, Yang H and Domingos J.B. 2012. Synthesis and Catalytic Properties of Silver Nanoparticle–Linear Polyethylene Imine Colloidal Systems. *J. Phys. Chem. C*, 116 (7), 4594–4604.
- [6] Shi Y, Wang X, Liu W, Yang T, Xu R and Yang F. 2013. Multilayer silver nanoparticles for light trapping in thin film solar cells. *J. Appl. Phys.* 113, 176101; <http://dx.doi.org/10.1063/1.4803676>.
- [7] Karni T.C, Langer R and Kohane D.S. 2012. The smartest materials: the future of nanoelectronics in medicine. *ACS Nano*, 6:6541–6545.
- [8] Prabhu S, Poulouse E.K. 2012. Silver nanoparticles: mechanism of antimicrobial action, synthesis, medical applications, and toxicity effects. *International Nano Letters*, 2(32) available at: <http://www.inl-journal.com/content/2/1/32>
- [9] Pourali P, Baserisalehi M, Afsharnezhad S, Behravan J, Ganjali R, Bahador N and Arabzadeh S. 2013. The effect of temperature on antibacterial activity of biosynthesized silver nanoparticles. *BioMetals*, 26(1), 189–196.
- [10] Singh R, Sahu S.K and Thangaraj M. 2014. Biosynthesis of Silver Nanoparticles by Marine Invertebrate (Polychaete) and Assessment of Its Efficacy against Human Pathogens. *J Nanoparticles*. vol 2014, Article ID 718240, 1-7. <http://dx.doi.org/10.1155/2014/718240>.
- [11] Ravindran A, Chandran P and Khan S.S. 2013. Biofunctionalized silver nanoparticles: advances and prospects. *Coll Surf B Biointerf*, 105: 342–352.
- [12] Singh C, Sharma V, Naik, P.R., Khandelwal V and Singh, H.A. 2011. Green biogenic approach for synthesis of gold and silver nanoparticles using *Zingiber officinale*. *Dig J Nanomaterials and Biostructures*. 6: 535–542.
- [13] Sastry M., Patil V and Sainkar S.R. 1998. Electrostatically Controlled Diffusion of Carboxylic Acid Derivatized Silver Colloidal Particles in Thermally Evaporated Fatty Amine Films. *J. Phys. Chem. B*. 102: 1404–1410.
- [14] Mulvaney P. Surface plasmon spectroscopy of nanosized metal particles. 1996. *Langmuir*. 12: 788–800
- [15] Bindhu M.R and Umadev M. 2013. Synthesis of monodispersed silver nanoparticles using Hibiscus cannabinus leaf extract and its antimicrobial activity. *Spectrochimica Acta Part A-Molecular and Biomolecular Spectroscopy*. 101: 184–190.
- [16] Shahverdi A.R, Fakhimi A, Shahverdi H.R and Minaian MS. 2007. Synthesis and effect of silver nanoparticles on the antibacterial activity of different antibiotics against *Staphylococcus aureus* and *Escherichia coli*. *Nanomedicine*. 3: 168–171.
- [17] Bao L, Deng A, Li Z, Du G and Qin H. 2010. Chemical constituents of rhizomes of *Zingiber officinale*. *Zhongguo Zhong Yao Za Zhi*. 35: 598–601.
- [18] Geetha N, Geetha T.S, Manonmani P, Thiyagarajan M. 2014. Green Synthesis of Silver Nanoparticles Using *Cymbopogon Citratus* (De) Stapf. Extract and Its Antibacterial Activity. *Australian J Basic and App Sci*, 8(3), 324–331.
- [19] Rodríguez-León E, Iñiguez-Palomares R, Navarro R.E, Herrera-Urbina R, Tánori J, Iñiguez-Palomares C and Maldonado A. 2013. Synthesis of silver *Claudia* nanoparticles using reducing agents obtained from natural sources (*Rumex hymenosepalus* extracts). *Nanoscale Research Letters*, 8:318. <http://www.nanoscalereslett.com/content/8/1/318>.
- [20] Zhang H, Wu M, Sen A: In *Nano-Antimicrobials: Silver Nanoparticle Antimicrobials and Related Materials*. Cioffi N, Rai M.(eds) New York: Springer; 2012:3–45.
- [21] Niraimathi K.L, Sudha V, Lavanya R and Brindha P. 2013. Biosynthesis of silver nanoparticles using *Alternanthera sessilis* (Linn.) extract and their antimicrobial, antioxidant activities. *Coll Surf B Biointerf*. 102:288–291.
- [22] Otari S.V, Patil R.M, Ghosh S.J, Thorat N.D and Pawar S. H. 2015. Intracellular synthesis of silver nanoparticle by actinobacteria and its antimicrobial activity. *Spectrochimica Acta Part A: Molecular and Biomolecular Spectroscopy* 136:1175–1180.